

Disassembly and Degradation of Photosystem I in an *in Vitro* System Are Multievent, Metal-dependent Processes*

Received for publication, April 24, 2003, and in revised form, July 17, 2003
Published, JBC Papers in Press, July 28, 2003, DOI 10.1074/jbc.M304299200

J. Nathan Henderson‡, Jianying Zhang, B. Walter Evans, and Kevin Redding§

From the Departments of Chemistry and Biological Sciences, University of Alabama, Tuscaloosa, Alabama 35487-0336

An *in vitro* system was created to study the process of membrane protein degradation by using photosystem I (PS1) as a model membrane protein. Purified chloroplast membranes were incubated at 30 °C in a defined buffer along with various extracts or reagents to reconstitute the disassembly and degradation of PS1, which was monitored by a variety of techniques that probe the integrity of the PS1 complex: photo-biochemical assays, semi-native gel electrophoresis, low temperature fluorescence spectroscopy, and immunoblots using antibodies against different PS1 subunits. During a typical time course, degradation of PS1 appeared to be a multievent process, with disassembly of the complex preceding proteolysis of the subunits. The first change seen was a rapid (<5 min) decrease in PS1 photochemical activity. This was followed by a diminution of far-red fluorescence emission from the core antenna of PS1 and a slower disassembly of the PS1 chlorophyll-protein core complex, as visualized by semi-native gel electrophoresis. Surprisingly, the latter was not accompanied by a similar rate of proteolysis of the PsaA core subunit. In contrast, addition of soluble proteases caused rapid loss of immuno-detectable PS1 polypeptides and cleavage of the major PS1 polypeptides in interhelical loops. The *in vitro* degradation process was time- and temperature-dependent but did not require ATP, GTP, or soluble chloroplast proteins. Chelation of divalent cations by EDTA inhibited the later steps of disassembly and proteolysis, and this effect could be reversed by addition of micromolar Zn²⁺, with Co²⁺ and Ca²⁺ providing somewhat lower activity.

Biological cells are dynamic structures in which nearly all the molecular components are in a state of continuous turnover. The turnover of molecular components continues even when the cell is not undergoing active growth (1). Steady-state protein concentration in the cell is determined by the relative rates of protein synthesis and protein degradation (proteolysis). Modulation of these processes can have dramatic effects on the abundance of individual cellular proteins, converting a stable protein into a short lived one and vice versa. Intracellular proteases play a major role in controlling protein abundance, as well as clearing damaged and misfolded proteins from the cell.

* This work was supported by NIGMS Grant GM66345-01 from the National Institutes of Health. The costs of publication of this article were defrayed in part by the payment of page charges. This article must therefore be hereby marked "advertisement" in accordance with 18 U.S.C. Section 1734 solely to indicate this fact.

‡ Present address: Dept. of Chemistry, University of Oregon, Eugene, OR 97403-1253.

§ To whom all correspondence should be addressed: Depts. of Chemistry and Biological Sciences, University of Alabama, 120 Lloyd Hall, 6th Ave., Tuscaloosa, AL 35487-0336. Tel.: 205-348-8430; Fax: 205-348-9104; E-mail: Kevin.Redding@ua.edu.

Much is known about the regulated degradation of proteins in several systems. Eukaryotic proteolytic systems include lysosomal proteases and the well characterized ubiquitin/proteasome pathway (2). In the latter, proteins are targeted for degradation by covalent linkage of the carboxyl-terminal glycine of ubiquitin to the ϵ -amino group of specific lysines in the target protein. In general, poly-ubiquitination targets these proteins for ATP-dependent degradation by a complex of enzymes known as the proteasome (3). Examples of proteolytic systems of prokaryotic origin include the ATP-dependent FtsH, Lon, and ClpP proteases and the ATP-independent DegP protease. Substrates of these systems are continuing to be identified; however, most of what is known about the mechanisms of protein degradation comes from examples where the substrate is a soluble protein. Less is understood about how integral membrane proteins are degraded. This has been due in part to the intrinsic difficulty of working with membrane proteins, along with a lack of probes for the integrity of the polypeptide structure within the lipid bilayer. What remains unclear is how proteolytic systems are able to degrade the hydrophobic, integral membrane portions of membrane proteins.

Membrane proteins are involved in many vital biological functions, such as signal transduction, ion and metabolite transport, energy conversion, and structural support. Because of the many important functions of membrane proteins as well as the existence of several disease states associated with membrane protein function gone awry (4–8), understanding how these proteins are degraded has become a topic of considerable interest in recent years. Membrane proteins often exist as multisubunit complexes, and it is well known that the inefficient assembly of complexes or defects in a single subunit of the complex can lead to the degradation of all the subunits of the complexes. The four major membrane protein complexes located in the chloroplast thylakoid membrane of green plants, photosystem II (PS2),¹ cytochrome *b₆f*, photosystem I (PS1), and ATP synthase, all exhibit this phenomenon (9, 10). This has led to the idea that the chloroplast possesses a "quality control" system that is responsible for assessing the integrity of these complexes and targeting the aberrant ones for degradation. Not much is known about the mechanisms used to recognize aberrant membrane proteins in the chloroplast; however, the identities of several chloroplast proteases (ClpP, DegP, FtsH, SppA, and Lon) have been revealed recently by genomic sequencing and biochemical and molecular techniques (11–18). Furthermore, several reports indicate that some of these proteases are involved in the degradation of thylakoid membrane

¹ The abbreviations used are: PS2, photosystem II; Chl, chlorophyll; CP1, chlorophyll-protein complex 1; CP2, chlorophyll-protein complex 2; DTT, dithiothreitol; EDTA, ethylenediamine tetra-acetic acid; DEPC, diethyl pyrocarbonate; LHC, light harvesting complex; NEM, *N*-ethylmaleimide; PS1, photosystem I; TAP, Tris-acetate-phosphate medium; BisTris, 2-[bis(2-hydroxyethyl)amino]-2-(hydroxymethyl)propane-1,3-diol.

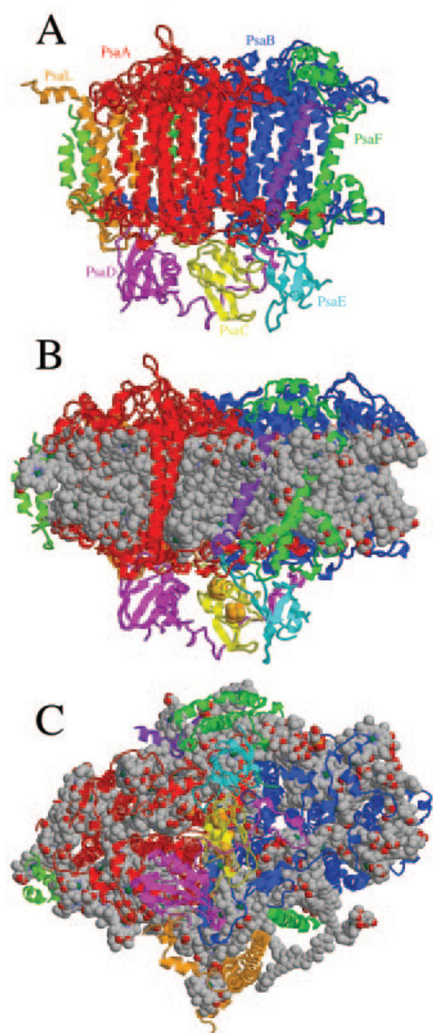


FIG. 1. PS1 structural arrangement, based on the 2.5-Å structural coordinates (24). A, cofactors have been omitted for clarity. Polypeptides are shown as ribbon models using the following color scheme: red (PsaA), blue (PsaB), yellow (PsaC), magenta (PsaD), cyan (PsaE), green (PsaF, PsaI, PsaK), purple (PsaJ), and orange (PsaL). B, similar view, but with cofactors depicted as space-filling models (C = gray, N = blue, O = red, Mg = green, S = yellow, Fe = orange). C, view from B rotated 90° to see the stromal side of PS1.

protein complexes. The soluble stromal protease ClpP is thought to participate in the *in vivo* degradation of the large membrane-bound cytochrome *b₆f* complex (19) and PS2 (20). The membrane-bound ATP- and Zn²⁺-dependent FtsH protease has also been implicated in some aspects of PS2 degradation (21) as well as the light-stimulated degradation of unassembled Rieske FeS protein (22). In *Escherichia coli*, FtsH reportedly degrades several integral membrane proteins in a processive manner (23).

Although the light-dependent degradation of PS2 during photoinhibition has received much attention, much less is known about the degradation of PS1. However, PS1 could serve as an excellent model for the study of membrane protein degradation for several reasons. 1) A crystal structure at 2.5 Å resolution is available for the cyanobacterial PS1 (24) (Fig. 1). 2) The vast majority of the functional parts of PS1 are in the integral membrane portions of the protein, unlike many membrane proteins, which are basically soluble proteins anchored to the membrane by one transmembrane α -helix. 3) PS1 has many cofactors (~100 chlorophyll molecules (Chl), 8 carotenoids, 2 phylloquinones, and 3 Fe₄S₄ clusters), which can serve

as built-in spectroscopic probes for the structure of the protein. The core of PS1 is composed of the heterodimeric proteins PsaA and PsaB; both have molecular masses around 82 kDa and possess 11 transmembrane α -helices. The first 6 transmembrane α -helices of PsaA and PsaB bind chlorophylls that serve as the "core" antenna, while the last 5 form a cage around all but 2 of the cofactors involved in photochemistry. Electron transfer through PS1 begins with the excitation of P₇₀₀, which then transfers an electron to a nearby Chl generating a charge-separated state (P₇₀₀⁺ Chl⁻). This state is further stabilized by the transfer of the electron to the phylloquinone and then finally to the iron-sulfur clusters. The iron-sulfur clusters are then oxidized by the soluble ferredoxin, and the system is re-set by the reduction of P₇₀₀⁺ by the luminal protein plastocyanin. The subunits PsaC, PsaD, and PsaE form the docking site for ferredoxin on the stromal side of PS1, and PsaF (along with PsaA/B) forms the docking site for plastocyanin in the lumen. Fig. 1 illustrates the structure of PS1. Another class of thylakoid membrane proteins important in photosynthesis are the light harvesting complexes (LHC). Each LHC polypeptide contains 3 transmembrane α -helices binding 13 chlorophylls and 2 carotenoids. They are often referred to as the peripheral antenna of PS1 because they function in funneling the excitation energy from light to the core antenna of PS1 and on to P₇₀₀.

EXPERIMENTAL PROCEDURES

Algal Strain Growth and Chloroplast Membrane Purification—All experiments shown in this paper made use of the *cw10* (cell wall-less) strain CC-849 (*Chlamydomonas* Genetics Center; Duke University). Algae were grown photoheterotrophically at 25 °C in well aerated liquid TAP medium (25) containing 50 mM sorbitol to a concentration of 2–4 × 10⁶ cells/ml in a volume of ~3 liters. Cells were centrifuged at 2300 × *g* for 10 min in a GS-3 rotor at 4 °C and resuspended at 2 × 10⁸ cells/ml in Breaking buffer (0.3 M sorbitol, 50 mM HEPES-KOH, pH 7.8, and 5 mM MgCl₂). The cells were then lysed gently by addition of concentrated saponin to 0.25% final concentration, followed by incubation for 10 min on ice. From this point on, material was kept at 0–4 °C. Chloroplasts were harvested by centrifugation at 2300 × *g* for 1 min in an SS-34 rotor. The pellet was resuspended in 24 ml of Breaking buffer at 4 °C, and two 12-ml portions were loaded on top of 12 ml of 45% Centricoll in Breaking buffer. After centrifugation for 20 min in a Beckman SW-28 swinging bucket rotor at 4600 × *g*, whole chloroplasts were removed from the top of the 45% Centricoll layer, diluted with 3 volumes of Breaking buffer, and collected by spinning at 1500 × *g* for 5 min in a Sorvall SS-34 rotor. The supernatant was removed, and the chloroplasts were lysed hypotonically by resuspension with 10 times the pellet volume of Lysis buffer (10 mM HEPES-KOH, pH 7.8, 5 mM MgCl₂, 1 mM dithiothreitol (DTT)). Membranes and stroma were separated by centrifugation for 20 min at 265,000 × *g* in a Ti-70 rotor. Supernatant containing stromal material was removed, and the pellet was resuspended in a minimum volume of Lysis buffer; glycerol (20% final concentration) was added to both stromal and membrane fractions. Separate aliquots were frozen with liquid nitrogen and stored at –80 °C. Chlorophyll concentration was measured as described by Porra *et al.* (26).

In Vitro Degradation Assays—Chloroplast membranes were centrifuged and resuspended in Reaction buffer (25 mM HEPES-KOH, pH 7.8, 5 mM MgCl₂, 2 mM CaCl₂, 10 μM ZnCl₂, and 0.5 mM DTT) on ice at a concentration of 0.1 mg of Chl/ml. Degradation assays were initiated by transfer to 30 °C, and samples were taken over time, as detailed below.

PS1 Photochemical Assays—At each time point, 600 μl of sample (60 μg of Chl) was removed, centrifuged at 21,000 × *g* for 2 min, and resuspended in 80 μl of buffer HE (5 mM HEPES-KOH, pH 7.5, 10 mM EDTA) + 20% glycerol, frozen in liquid N₂, and stored at –80 °C for subsequent O₂ uptake measurements. A Clark-type oxygen electrode was used to measure O₂ uptake rates essentially as described (27), using a red LED as actinic light source. Double-reciprocal plots were used to estimate the maximal velocity of O₂ uptake.

Low-Temperature Fluorescence Spectroscopy—At each time point, 7.5 μl (0.75 μg of Chl) was removed and mixed well with 242.5 μl of HE buffer containing 60% glycerol and 5 μg/ml B-phycoerythrin (*Porphyridium cruentum*; Sigma). The mixtures were transferred to quartz tubes (5-mm diameter) and immediately frozen in liquid N₂ and stored at –80 °C for subsequent low-temperature fluorescence measurements.

These were performed at 77 K using a Dewar that holds the quartz tubes in the excitation beam path while bathed in liquid N₂. Fluorescence emission spectra were collected with a FLUOROMAX-3 spectrofluorometer between 550 and 750 nm using excitation at 467 nm.

Green Gels and Protein Gels—At each time point, 500 μ l of sample (50 μ g of Chl) was removed and centrifuged for 2 min at 21,000 \times *g*. After removal of the supernatant, the pellet was frozen with liquid N₂ and stored at -80 °C for subsequent green gel analysis. Membranes were resuspended with 50 μ l of loading buffer (50 mM Tris-HCl (2-amino-2-(hydroxymethyl)-1,3-propanediol), pH 6.8, 12% sucrose, 2% SDS) at 1 mg of Chl/ml, incubated at room temperature for 2 min, and then centrifuged at 21,000 \times *g* for 5 min at room temperature. Twenty μ g of chlorophyll was loaded in each lane of an SDS-polyacrylamide gel (4% stacking and 10% resolving) and run at 12 V cm⁻¹ for 3 h. Images were obtained with a Fluor-S MultiImager (Bio-Rad) using white light and a red filter to reduce background; quantification of optical densities was performed using Bio-Rad Quantity One software.

For analysis of CP1 polypeptides, the CP1 band was carefully cut out of the gel and frozen in liquid nitrogen. After thawing on ice, the gel slice was ground in 10 μ l of 2 \times Laemmli buffer (4 M urea, 4% SDS, 20% glycerol, 125 mM Tris-HCl, pH 6.8), followed by addition of 80 μ l of 1 \times Laemmli buffer and careful mixing. After incubation at 50 °C for 15 min and centrifugation at 21,000 \times *g* for 5 min, 30 μ l of supernatant was loaded onto a 4–20% Tris-glycine gel (Invitrogen). After electrophoresis for 5 h at 12 V cm⁻¹ using 0.05% SDS in the running buffer, the gel was stained with SYPRO Orange (Molecular Probes) according to the manufacturer's instructions and photographed with the MultiImager using shortwave UV excitation and a 520-nm low-pass filter.

Immunoblot Analysis—At each time point, 10 μ l of sample (1 μ g of Chl) was removed and placed into tubes containing 10 μ l of 4 \times SDS-Loading buffer (8% SDS, 40% glycerol, 1 M Tris-HCl, 2 mM EDTA, 0.005% bromophenol blue), 19 μ l of H₂O, and 1 μ l of 1 M DTT. The samples were immediately vortexed, frozen with liquid N₂, and stored at -80 °C for subsequent immunoblot analysis. Samples were solubilized by incubation at 37 °C for 30 min and centrifuged at 21,000 \times *g* for 5 min, and 10 μ l of supernatant (250 ng Chl) was loaded onto a 4–12% BisTris gel (NuPAGE). The resolved proteins were transferred electrophoretically onto Millipore Immobilon-P polyvinylidene fluoride membranes. Immunoblots were performed as described using antibodies raised from rabbits against PsaA, PsaD, and PsaF (28). Chemiluminescence was imaged and quantified with a Fluor-S MultiImager using Quantity One software (Bio-Rad).

RESULTS

The initial experiments in this study involved incubation of PS1-containing membranes in reaction buffer for variable lengths of time to determine the *in vitro* activity endogenous to the membranes. Purified chloroplast membranes were used to minimize the possibility of artifactual proteolysis arising from proteases normally located in other cellular compartments. Several different techniques were used to follow the degradation of PS1.

O₂ Polarography—A Clark-type O₂ electrode (29) was used to monitor PS1 photochemical activity after various lengths of incubation *in vitro*. Ascorbate served as an electron donor to P₇₀₀, and reduction of O₂ (to O₂⁻) was mediated by methyl viologen. The rate of PS1-dependent O₂ reduction was measured at different light fluxes by subtracting the dark rates from the light rates, and double-reciprocal plots allowed calculation of the maximal rate. The rates of O₂ uptake are plotted *versus* light intensity in Fig. 2. It is clear that there were two light-dependent O₂ reduction activities, a saturable activity (PS1) and a non-saturable activity. The latter is non-enzymatic and has been described before (30). As the length of incubation increased, the overall rate of O₂ uptake decreased until, after 40–60 min, the saturable activity was practically gone, although the non-saturable activity persisted (Fig. 2; see Fig. 6).

Low-Temperature Fluorescence—Association of chlorophylls with the polypeptides of PS1 significantly shifts their fluorescence emission to the red, allowing them to serve as spectroscopic reporters for the structure of the protein at the level of the lipid bilayer. It is necessary to collect spectra at cryogenic temperatures to see PS1 fluorescence (29). Fluorescence spec-

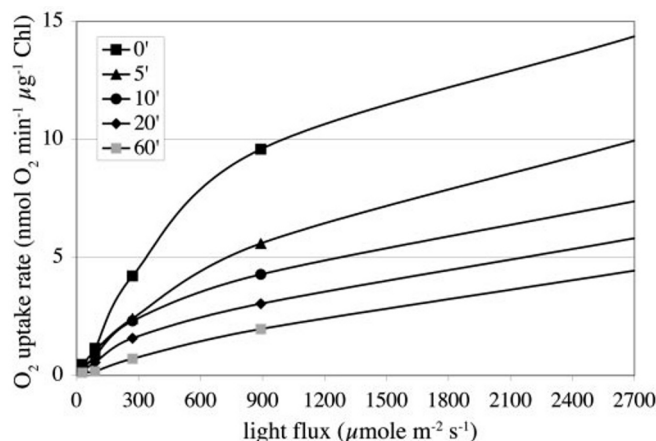


Fig. 2. **Photochemical assays.** After increasing times of incubation, membranes were washed and assayed for photochemical activity at a range of light intensities. Rates are reported as light-dependent O₂ uptake (using methyl viologen as a mediator), normalized to Chl content.

tra of chloroplast membranes incubated for various lengths of time in the *in vitro* system are shown in Fig. 3. The primary features of the emission spectra are peaks at 685 and 695 nm and a shoulder centered at 711–712 nm and trailing further into the red. The first two peaks are due to the PS2 antenna chlorophylls, although the broad red band corresponds to PS1 antenna chlorophylls (31). Within 10–20 min of incubation, the fluorescence emission from PS1 dropped by 25–50% (Fig. 3; see Fig. 6), along with PS2 fluorescence, and continued to decline steadily out to 90 min, leaving a broad, featureless peak centered around 682 nm. This steady loss of fluorescence from protein-associated chlorophylls was accompanied by an increase in the fluorescence from free chlorophylls at 660 nm (Fig. 3), whose intensity was somewhat variable.

Green Gels—A form of semi-native gel electrophoresis, often referred to as “green gels,” was used to assess the integrity of the PS1 core complex after various lengths of incubation *in vitro*. Gentle solubilization of chloroplast membranes releases PS1 sub-complexes (CP1), containing the core subunits PsaA and PsaB along with most of their associated chlorophylls, as well as chlorophyll-containing LHC complexes (CP2) from the membrane (32). Following SDS-PAGE at low-temperature, complexes are easily visualized as green bands. Disappearance of both the CP1 and CP2 complexes occurred progressively over time (Fig. 4), and they had dropped by more than 70% after 90 min (see Fig. 6).

Immunoblots—Immunoblots were performed to follow proteolysis of the PsaA and PsaD subunits. These serve as representative core and peripheral subunits, and the antibodies used to detect them gave strong, specific signals. An immunoblot from the initial experiment is shown in Fig. 5. Relative to the rate of disappearance of the CP1 band in Fig. 4, proteolysis of the PsaA and PsaD subunits seemed to be much slower. In particular, degradation of PsaD was minimal (5–10%) after 90 min, although PsaA experienced greater degradation (~40%). Also, a more slowly migrating band with an apparent molecular mass of 115 kDa accumulated at the later time points (Fig. 5). Additional experiments indicated that PsaD was fairly stable even after 16 h of incubation (see below), although proteolysis of the small intrinsic PsaF subunit (see Fig. 1) seemed to occur with similar kinetics as that of PsaA (data not shown).

Given the apparently higher rate of proteolysis of PsaA compared with PsaD, it was of interest to determine whether or not PsaD had been removed from the membrane, because degradation of PsaA might cause PsaD to be released from the

FIG. 3. Normalized low temperature fluorescence emission spectra of chloroplast membranes after various times of incubation. Peaks corresponding to free chlorophyll, PS2, and PS1 are indicated. Spectra after different times of incubation are indicated as follows: 0 min (black squares), 10 min (black diamonds), 20 min (black triangles), 40 min (black circles), 60 min (dark gray squares), 90 min (gray circles).

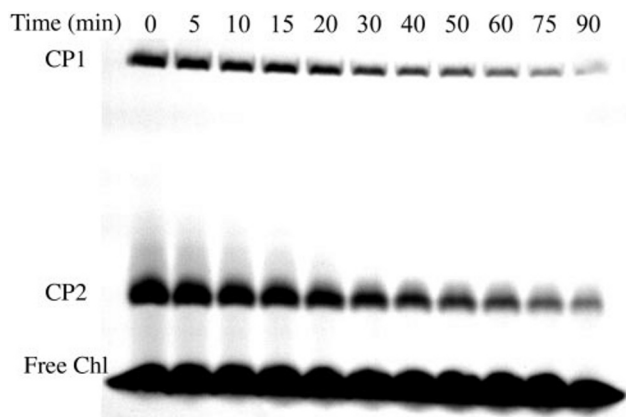
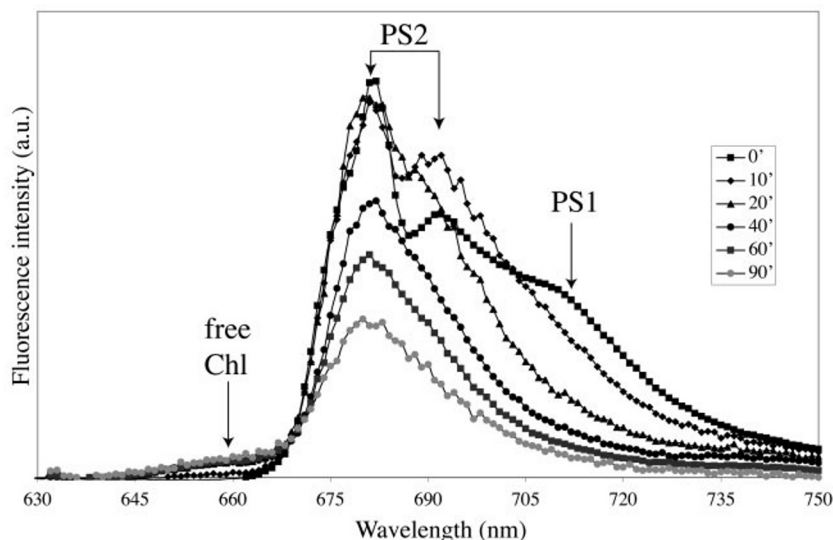


FIG. 4. Disappearance of the PS1 complex. Semi-native SDS-PAGE was performed using chloroplast membranes that had been incubated in the *in vitro* system for various times. The position of the PsaA/PsaB heterodimer (CP1) and the LHC complexes (CP2) are indicated.

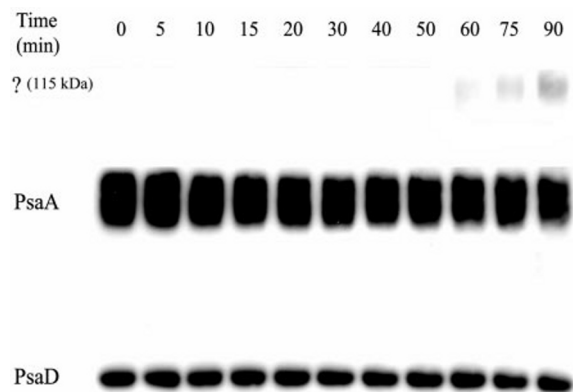


FIG. 5. Slow proteolysis of PS1 subunits. After various times of incubation, chloroplast membranes were dissolved in SDS-PAGE sample buffer; equal volumes (corresponding to 250 ng of input Chl) were loaded on the gel, blotted, and probed with antibodies against PsaA and PsaD. A cross-reactive polypeptide of 115-kDa apparent molecular weight appeared late in the time course and is marked as ?.

membrane. In order to test this, samples were separated into pellet and supernatant fractions after incubation and separately solubilized for immunoblot analysis. Surprisingly, the PsaD subunit was found exclusively in the pellet throughout a

90-min time course, during which ~40–50% of the PsaA subunit was degraded (data not shown)

Summary of Activity—Time courses such as that shown in Figs. 2–5 were run on different chloroplast preparations, and the degradation activity was quite reproducible. Results from several such time courses were quantified and averaged to produce Fig. 6. The drop in PS1 photochemical activity was the most rapid event, with maximum activity down to roughly 50% within 5 min of incubation, followed by a more gradual decrease. The next most rapid process was the drop in chlorophyll fluorescence from PS1, indicative of perturbation of pigment-protein contacts. The fact that it was not matched by a corresponding rise in fluorescence from free chlorophylls does not lend support to the idea that pigments were being removed from the proteins. The decrease in CP1 and PsaA was steady over the time courses, with the former dropping faster. Taken together, these data would indicate that the process we observe *in vitro* is primary disassembly, rather than degradation, of PS1. Proteolysis of the subunits is relatively slow in this *in vitro* system, although it was significantly faster than proteolysis of PsaA *in vivo*, where its half-life is 18–24 h (data not shown).

PS1 Degradation in Whole and Lysed Chloroplasts—In order to address the physiological relevance of the *in vitro* system, degradation of PS1 was examined in both lysed chloroplast membranes and whole chloroplasts. Freshly isolated chloroplasts were divided, and half were immediately lysed hypotonically, although the other half were left intact. Both were re-suspended in reaction buffer and incubated for various times. The integrity of the whole chloroplasts was inspected microscopically after each time point had been reached; even after 90 min of incubation, the whole chloroplasts remained intact (data not shown). By using all four techniques, there was little difference in the rate or extent of PS1 degradation in lysed *versus* whole chloroplasts. In both cases, the results resembled those of the initial experiments described in Figs. 2–6 (data not shown). Because of this and the ease of manipulation of the lysed membranes, all further experiments were performed in this system.

Temperature Dependence of PS1 Degradation—In order to assess the dependence of the degradation activity upon temperature, 100-min end point assays were performed at temperatures ranging from 0 to 30 °C. The results are presented in Fig. 7. There was essentially no PS1 degradation after 100 min at 0 °C, as these samples resembled the 0-min time point (data not shown). Degradation was almost undetectable at 10 °C,

FIG. 6. **Quantitative summary of PS1 degradation time courses.** Each curve contains data from several experiments like those shown in Figs. 2–5 ($n = 3$ for photochemical activity; $n > 5$ for all others; the bars are 1 S.D.). Using double-reciprocal plots, the maximal velocity of O_2 uptake (triangles) was determined after each incubation time. The average and standard deviation from 3 separate experiments is shown along with a fit to a bi-exponential decay ($A_1 = 49\%$, $\tau_1 = 1.7$ min, $A_2 = 38\%$, $\tau_2 = 23$ min). Normalized low temperature fluorescence emission (circles) was integrated in the 710–713-nm range. The CP1 band (diamonds) was quantified by its absorbance in the red region. The level of PsaA (squares) was measured immunologically, as in Fig. 5.

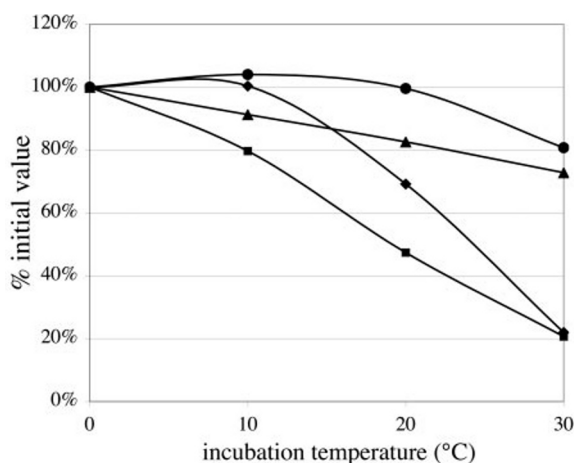
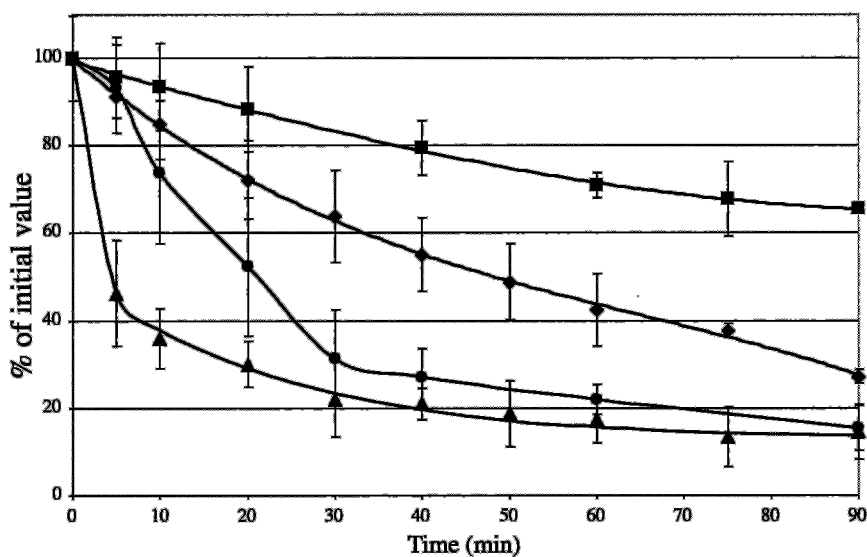


FIG. 7. **Temperature dependence of PS1 degradation activity.** After 100 min of incubation at 0, 10, 20, or 30 °C, samples were analyzed by various techniques. Low temperature fluorescence (squares), CP1 (diamonds), PsaA (triangles), and PsaD (circles) were quantified as described in the legend to Fig. 6.

except for a small (~20%) drop in far-red fluorescence. Far-red fluorescence dropped much more at 20 °C (~55%) and 30 °C (~80%). The chlorophyll-protein complex CP1 dropped by 30 or 80% at 20 or 30 °C, respectively. Degradation of PsaD was not detectable under 30 °C. Accumulation of the 115-kDa band was barely detectable after 100 min at 20 °C and became more pronounced at 30 °C (data not shown).

Addition of Soluble Proteases—To test whether or not PsaA and PsaD were intrinsically stable to proteolysis and to model what might be expected upon the addition of stroma, membranes were incubated in the presence or absence of trypsin and chymotrypsin for various lengths of time. As expected, disappearance of immunoreactive PsaA and PsaD bands was greatly enhanced by the addition of proteases (Fig. 8A); within 10 min, the vast majority of full-length PsaA and PsaD had disappeared. In contrast, disappearance of CP1 and CP2 was accelerated only slightly by the presence of proteases, although they caused a readily discernible increase in migration rate within 10 min, probably by removal of peripheral subunits or extramembranous portions of core subunits (Fig. 8B). In addition, the slowly migrating 115-kDa band, often seen accumulating at the later time points, did not accumulate in the presence of proteases, indicating that it may be particularly

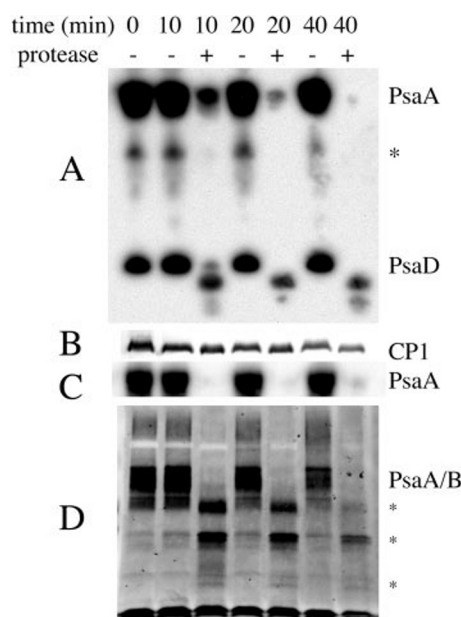


FIG. 8. **Effect of added trypsin and chymotrypsin.** Incubations were carried out for various lengths of time with or without addition of 120 units of trypsin and 0.3 units of chymotrypsin. At the end of each time point, samples were placed on ice with a 2-fold excess of bovine pancreatic trypsin inhibitor and were then subjected to immunoblot (A) and green gel (B) analysis. The CP1 bands were cut out of the gel; proteins were extracted from them and submitted to SDS-PAGE followed by either anti-PsaA immunoblot (C) or SYPRO-Orange staining for total protein (D). The position of the PsaA/PsaB bands, as well as some new bands created by proteolysis (*), are indicated in D.

protease-sensitive. Very similar results were obtained with protease K (data not shown).

We hypothesized that the apparent discrepancy between the immunoblot and green gel results stemmed from the fact that these soluble proteases could only hydrolyze peptide bonds in the interhelical loops (in the case of PsaA) or parts of the polypeptide that were not tightly folded. Whereas such proteolysis would cause disappearance or shifts in the immunoreactive bands, it would not necessarily cause dissolution of the CP1 complex, which would be held together primarily by hydrophobic interactions. To test this hypothesis, we isolated the CP1 bands from the green gel, extracted proteins with SDS solubilization buffer, and analyzed the extracts by immunoblot and SDS-PAGE. The immunoblot showed no apparent PsaA in

TABLE I
Summary of results from inhibitors

The inhibitors, concentrations used, class of protease inhibited (or residue modified) are indicated. Each was added at the concentration indicated for a 2-h incubation. Activity was calculated as a fraction of the amount of PsaA degraded in a reaction without inhibitors.

Inhibitor	Concentration used	Protease inhibited or residue affected	% Activity
EDTA	10 mM	Metallo	39
1,10-Phenanthroline	5 mM	Metallo	104
Benzamidine-HCl	1 mM	Serine	100
Phenylmethanesulfonyl fluoride	1 mM	Serine	98
ϵ -Aminocaproic acid	10 mM	Serine	101
Di-isopropylfluorophosphate	0.1 mM	Serine	104
3,4-Dichloroisocoumarin	0.1 mM	Serine	109
Leupeptin	20 μ g/ μ l	Serine	102
E64	20 μ M	Cysteine	108
Pepstatin A	25 μ M	Aspartic	104
Diethyl pyrocarbonate	12 mM	Catalytic His	103
<i>N</i> -Ethylmaleimide	0.1 mM	Catalytic Cys	99
Apayrase	33 units/ml	ATP-dependent (hydrolyzes ATP)	85

the CP1 complexes isolated after trypsin treatment, but the amount of PsaA in the nontreated CP1 complexes correlated with the amount of CP1. The lack of PsaD (data not shown) even in the absence of proteases is probably due to its absence in CP1. When total proteins from CP1 were stained with the fluorescent protein dye, SYPRO Orange, the PsaA/PsaB bands were easily visible as the major polypeptides of CP1. Even after 10 min in trypsin, these had been clipped to two major bands and perhaps several smaller bands. Thus, these bands do not contain the epitopes recognized by our anti-PsaA antibody.

Attempts to Stimulate PS1 Degradation—Several attempts were made to stimulate the degradation process using several independently prepared stromal extracts. No effect was seen upon addition of stromal extracts (1.5 mg/ml protein) or 5 mM ATP and/or GTP. Pretreatment of the membranes for 1 h with light (1300 microeinsteins/m²/s at 630–670 nm) on ice in the presence or absence of artificial electron donors also had no effect (data not shown). In addition, no combination of stroma, nucleotides, and light pretreatment resulted in stimulation of activity (data not shown).

Effect of Inhibitors—Various protease inhibitors were added to the *in vitro* assay in order to identify the class(es) of protease(s) involved. The results are summarized in Table I. Only EDTA caused significant inhibition. Accumulation of the 115-kDa band was also blocked in the presence of EDTA (data not shown).

The effect of EDTA was characterized in more detail by running *in vitro* time courses with and without EDTA (Fig. 9). The presence of EDTA in the *in vitro* assay blocked much of the initial drop in maximal PS1 photochemical activity, and the activity remained higher over time (Fig. 9A). After 60 min with EDTA, during which time the loss of far-red fluorescence and increase in free chlorophyll fluorescence were nearly complete under normal conditions, the fluorescence emission spectrum changed very little (Fig. 9B). The CP1 and CP2 complexes were stable in membranes incubated with EDTA up to 4 h, a time sufficient to allow almost complete loss in the absence of the chelator (Fig. 9C). Thus, EDTA inhibits disassembly as well as proteolysis. In order to observe complete proteolysis of PsaA, the time course was extended to 16 h (Fig. 9D). PsaA was not indefinitely stable in the presence of EDTA, as there was some degradation of PsaA (45%) after 16 h. Degradation of the normally stable PsaD subunit after 16 h of incubation was 50% complete in the absence of EDTA and only 10% in the presence of EDTA.

Metal Reconstitution—The inhibition caused by EDTA was not dependent upon its presence in the reaction. If it was removed by washing several times with a buffer containing no metals or EDTA, activity was not restored (see Fig. 10). This

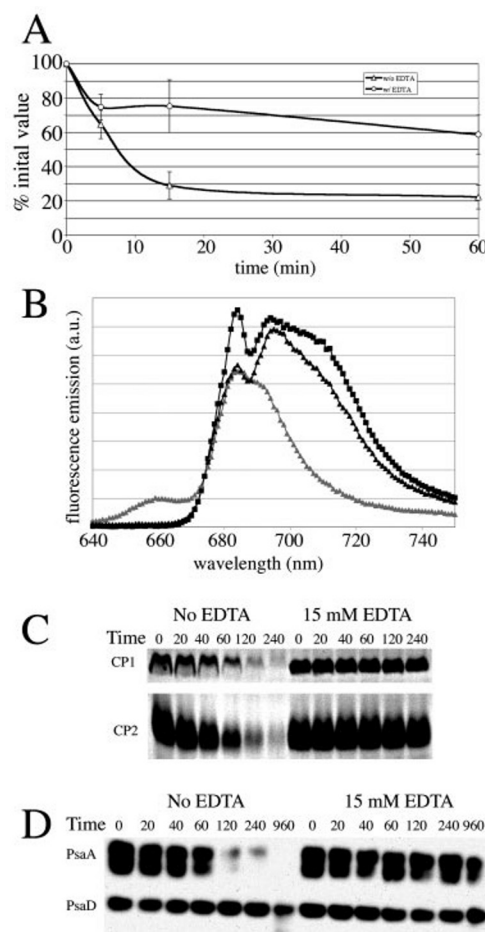


FIG. 9. Time courses in the presence of EDTA. A, photochemical activity in the absence (triangles) or presence of 15 mM EDTA (circles). B, low temperature fluorescence after 0 (black squares) or 60 min (black triangles) in the presence of 15 mM EDTA or after 60 min in the absence of EDTA (gray triangles). C, green gel of 4-h time course performed in the absence or presence of 15 mM EDTA. D, immunoblot of 16-h time courses performed in the absence or presence of 15 mM EDTA.

allowed the addition of metals back to the membranes to determine which ones could restore activity. We tested the alkali earth metals Mg²⁺ and Ca²⁺, as well as the transition metals Mn²⁺, Fe²⁺, Co²⁺, Ni²⁺, Cu²⁺, and Zn²⁺. Concentrations of each metal were varied over 4 orders of magnitude (1 μ M to 1 mM). An example of such an experiment is shown in Fig. 10, and a summary of all these experiments is presented in Table II. The ability of metals to restore activity followed this overall

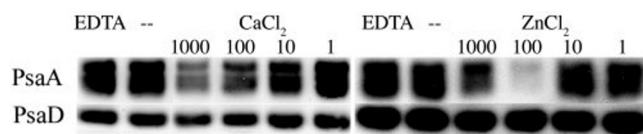


FIG. 10. Restoration of PsaA degradation activity with divalent cations after EDTA wash. Membranes were washed with 15 mM EDTA, and then the EDTA was washed out, and membranes were resuspended in reaction buffer containing no metals or EDTA. CaCl₂ or ZnCl₂ was added at 1 μM to 1 mM final concentration and membranes were incubated for 90 min. As controls, either no metals (-) or 15 mM EDTA were added.

trend: Zn²⁺ > Co²⁺, Ca²⁺ > Mn²⁺, Ni²⁺, Cu²⁺ > Fe²⁺, Mg²⁺. Zinc(II) restored the highest level of proteolytic activity (as observed by immunoblot) at a concentration of 100 μM; however, above this concentration it was inhibitory (Fig. 10). Interestingly, Cu²⁺ restored no activity at the concentrations below 1 mM, but at 1 mM a significant amount of activity was present. This is likely due to the presence in the reaction buffer of 0.5 mM DTT, which can reduce Cu²⁺ to Cu⁺; presumably, Cu⁺ is not active.

o-Phenanthroline is often used as a more specific chelator of Zn²⁺. Thus, it is surprising that it did not appear to act as an inhibitor in the assay (Table I). Further experiments established that *o*-phenanthroline could stimulate PS1 degradation, although the degradation activity still required metals (data not shown). This effect could be attributed to the hydrophobic character of phenanthroline, however, because a similar stimulatory effect was observed with phenanthrene (data not shown), which has a similar shape and hydrophobic character but cannot chelate metals.

Metal Ligand Modification—By having established the metal dependence of the process, the following question arose. What are the ligands for the metals? Side chains of cysteine and histidine residues often serve as ligands to metals like Zn(II). However, NEM and DEPC, which can modify cysteine and histidine residues, respectively, had no effect on the degradation activity (Table I). We hypothesized that binding to the metal might protect the ligands from modification. To test this idea, membranes were first washed with EDTA to remove the metals; the EDTA was then washed out using buffer without metals or DTT. The membranes were treated on ice with NEM or DEPC for 30 min, after which the reagents were washed off and the *in vitro* assay was carried out. Whereas DEPC displayed limited inhibition of PS1 degradation activity after the EDTA wash, NEM could inhibit much more strongly (Fig. 11). This suggests that essential cysteine, and perhaps histidine, residues had been modified, resulting in loss of enzymatic activity.

DISCUSSION

Degradation of PS1 in this *in vitro* system is a multievent process. Occurring within 5 min, the earliest change was a rapid decrease in the maximal rate of PS1 photochemical activity as measured by oxygen polarography (Fig. 6). Next, disruption of protein-chlorophyll contacts appears to occur, based on changes observed in low-temperature fluorescence spectra. The green gel (Fig. 4) showed steady loss of both CP1 and CP2 over time. Finally, immunoblots indicated that the disappearance of CP1 was not accompanied by a similar rate of PsaA and PsaD proteolysis (Fig. 5). In particular, degradation of PsaD was minimal, although PsaA degradation occurred somewhat more readily. Taken together, these results indicate that inactivation and disassembly of the PS1 complex occur before proteolysis of its subunits *in vitro*.

Several features of the *in vitro* system convince us that it represents a physiologically relevant process. The time courses

using the *in vitro* system appeared very similar to those using an *in organello* system (data not shown). The activity was time- and temperature-dependent. It was also metal-dependent and displayed specificity for specific metals (see below), which appeared to interact with cysteine and histidine side chains. One might suspect that what we have observed is simply PS1 “falling apart.” However, if that were the case, then one would expect that treatments that challenge the structural integrity of PS1 would accelerate its degradation. Instead, we found that treatment of thylakoid membranes with 6 M urea, which can remove peripheral stromal subunits from PS1 (33), resulted in less degradation activity (data not shown), as if the urea had inactivated protein(s) required for the activity. Also, PS1 purified from thylakoid membranes after extraction with the detergent β-dodecyl maltoside was much more stable than PS1 in intact thylakoid membranes (data not shown). One would expect that PS1 complexes in detergent micelles might be more susceptible to disintegration than those in a lipid bilayer; it appeared instead that removal of PS1 from the membrane separated it from the degradation activity. Finally, we have recently obtained *Chlamydomonas reinhardtii* mutants that suppress the enhanced degradation of some PS1 point mutants originally described in Ref. 27, and we have found that the PS1 degradation activity in membranes from these mutants is also diminished (data not shown). This argues that the activity that we observe *in vitro* is related to a process occurring *in vivo*.

We do not know exactly how PS1 photochemistry is inactivated, but it may involve a derangement of the iron-sulfur clusters bound by PsaC. These would seem to be the most likely electron transfer cofactors to be perturbed, because of their location on the periphery of PS1. We are currently testing this hypothesis using electron spin resonance spectroscopy. The changes in low-temperature fluorescence spectra and steady loss of CP1 should serve as good indicators of PS1 disassembly. As the length of *in vitro* incubation increases, fluorescence arising from PS1 (shoulder at 710–730 nm) decreased rapidly, although fluorescence at 660 nm, corresponding to free chlorophyll, appeared and increased steadily with time (Fig. 3 and data not shown). This suggests drastic changes in the organization of PS1 antenna chlorophylls, even complete removal of some of the chlorophylls from the PS1 complex. It is obvious from the spectra that the protein-chlorophyll interactions responsible for the red shift in chlorophyll fluorescence have been disrupted in some fashion. Likewise, loss of the CP1 chlorophyll-protein complex can be attributed to disassembly, as this technique measures the amount of chlorophyll associated with the complexes rather than the amount of the complex. The fact that CP1 is disappearing more rapidly than the PsaA polypeptide points either to the loss of chlorophyll from the complex or a decrease in the integrity of the assembled complex. Thus, CP1 disappearance does not seem to reflect the complete degradation of PS1 but is rather one of several events involved in the process. It is not surprising that PS1 disassembly precedes proteolysis of its subunits, as disassembly may render the complex susceptible to subsequent proteolysis. It seems that our *in vitro* system has not completely reconstituted the proteolytic activity, allowing the accumulation of partially disassembled complexes. It seems unlikely that such an accumulation would be allowed to occur *in vivo*, where disconnected chlorophylls could generate singlet oxygen and disassembled membrane proteins could interfere with thylakoid membrane function. Note that this loss of CP1 and low-temperature fluorescence is not due to wholesale destruction of chlorophylls, which decreased by no more than 5–10% over a 2-h time course (data not shown).

The observation that PsaD was degraded much more slowly

TABLE II
Summary of metal reconstitution data

Numbers in the table refer to the fold increase in the disappearance of CP1 (green gel), the ratio of phycoerythrin to PS1 fluorescence, and the disappearance of the PsaA band (immunoblot). All values refer to the activity of samples with 1 mM divalent cations relative to samples with no divalent cations added, except for Zn^{2+} , in which case it refers to the activity with 100 μM .

Technique	Metals used to reconstitute							
	Mg^{2+}	Ca^{2+}	Mn^{2+}	Fe^{2+}	Co^{2+}	Ni^{2+}	Cu^{2+}	Zn^{2+}
Green gel	1.1	2.7	2.0	1.1	2.6	1.6	1.7	2.3
Fluorescence	0.91	5.1	3.7	1.7	7.0	3.7	4.8	5.8
Immunoblots	0.95	2.6	1.6	1.1	2.0	1.1	0.98	5.8

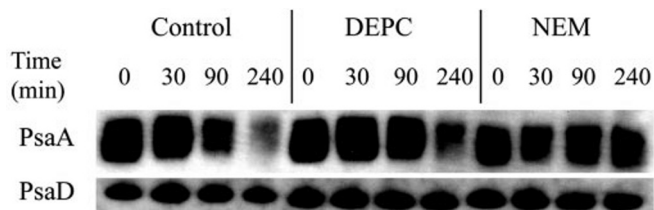


FIG. 11. **Inhibition by DEPC and NEM after EDTA pre-wash.** Chloroplast membranes were washed with 15 mM EDTA and then washed with buffer lacking EDTA, metals, or DTT. The membranes were treated on ice with buffer containing 100 μM NEM, 10 mM DEPC, or no additions (control) for 30 min and were then washed several times before the *in vitro* assay was carried out in the standard buffer (containing 2 mM Ca^{2+} and 10 μM Zn^{2+}).

than PsaA was surprising. Located on the stromal side of PS1, PsaC, PsaD, and PsaE are anchored to the membrane by the core subunits PsaA and PsaB. One would expect that destruction of the PsaA/PsaB core would release PsaD, along with the other peripheral subunits, from the complex and thus from the membrane. However, PsaD never seems to become soluble during the entire time course (data not shown). It was necessary to extend the time course to 16 h to see a significant amount of PsaD proteolysis (Fig. 9D). This suggests that either PsaD is an inherently stable protein and/or the proteases normally responsible for its degradation are largely absent in our *in vitro* system.

Even with the addition of nucleotide triphosphates, stromal extracts were unable to enhance any aspects of PS1 degradation over what was observed with membranes alone. Furthermore, we observed no significant difference in the rate or extent of PS1 degradation in lysed *versus* whole chloroplasts. Taken together, this indicates that the activity that we observe is localized to the thylakoid membrane. These results were somewhat surprising, given that ATP-dependent stromal proteases (e.g. Clp) reportedly play a role in the degradation of the membrane proteins PS2 and the cytochrome *b₆f* complex (18–20). The FtsH protease is an integral membrane protein, and an antibody against the *E. coli* protein (34) recognizes an ~75-kDa band in thylakoid membranes from *C. reinhardtii*,² similar to the size in *E. coli* (34) and in higher plant chloroplasts (12). It is possible that FtsH proteolytic activity, which is Zn^{2+} -dependent (35), is involved in proteolysis of PS1 subunits, but the ATPase activity is not required in this *in vitro* system. Degradation of the Rieske iron-sulfur protein of the cytochrome *b₆f* complex was also ATP-independent, despite the apparent involvement of FtsH (22). Whatever the identity of the membrane protein(s) required for PS1 degradation, it seems that they must be present in the same membrane as the substrate. Treatment of membranes with urea caused loss of degradation activity, which could not be complemented with added membranes from a PS1 null mutant (data not shown).

It is important to contrast action of the membrane-localized activity with what was observed using soluble proteases. Ad-

dition of trypsin and chymotrypsin proved that PsaA and PsaD are not inherently stable to proteolysis, and they could cause rapid apparent degradation of these polypeptides. However, comparison with the green gel allows one to conclude that they did not significantly accelerate the loss of the CP1 and CP2 complexes. This is likely explained by the restriction of their activity to the extra-membranous loops of an intact PS1 complex. Cleavage of such loops in the PsaA subunit followed by solubilization with SDS would result in several different smaller fragments, and this was observed upon extraction of proteins from the CP1 band (Fig. 8D). However, cleavage of extra-membranous loops would likely have little effect on the integrity of CP1, as it is held together by hydrophobic associations in the core of the complex. Thus, CP1 could run as a single band on the green gel despite the fact that cleavage of the extra-membranous loops had occurred. In fact, the action of proteases always produced a small shift in migration rate of CP1 (Fig. 8B and data not shown). Thus, the endogenous activity that we observe is quite different in its mode of action. The disassembly/degradation of PS1 may be an all-or-nothing event. If proteases had randomly clipped PS1 complexes here and there, we would have seen a gradual smearing and downshift of the CP1 band as it disappeared. This was not observed (Fig. 8B). Note also that we never observe discrete degradation products, either by immunoblot (Fig. 5) or in protein gels from extracted CP1 (Fig. 8D), although trypsin clearly produced such products (Fig. 8D). This suggests that the degradation activity is “processive.”

EDTA is a potent inhibitor of the disassembly and degradation activity. This implicates a membrane-bound metalloenzyme in the process of PS1 degradation and perhaps a metalloprotease. Over a 4-h time course, EDTA could completely inhibit changes in low temperature fluorescence spectra and loss of CP1, both indicative of PS1 disassembly. Whereas EDTA did not completely inhibit the rapid drop in maximal PS1 photochemical activity, the extent of the drop was lower, suggesting that this early event in PS1 degradation may be metal-independent and may be carried out by different agents than those involved in later steps. The effect of EDTA was clearly due to chelation and removal of essential metal(s), as it could be washed out without restoring activity. Reconstitution of EDTA-washed membranes with various metals revealed that proteolytic activity is fairly metal-specific ($Zn^{2+} > Co^{2+}$, $Ca^{2+} > Mn^{2+}$, Ni^{2+} , $Cu^{2+} > Fe^{2+}$, Mg^{2+}). Several studies report the replacement of native zinc ions from various metalloproteases with different divalent cations (36–40). One trend with these reconstitutions is that Co^{2+} commonly restores a higher level of activity than observed in the native enzyme. Although this is not the case with PsaA proteolysis, Co^{2+} did restore the highest level of PS1 disassembly, as indicated by low temperature fluorescence and green gel analysis (Table II). Cu^{2+} frequently restored high levels of activity as well. When chloroplast membranes were reconstituted with Cu^{2+} , the three lowest concentrations showed no activity, although the highest showed significant activity. This suggests that DTT, present at 0.5 mM, reduced Cu^{2+} to an inactive Cu^+ form, and that activity was restored only when the Cu^{2+} concentration

² J. Zhang and K. Redding, unpublished data.

exceeded the DTT concentration. Mn²⁺ and Ni²⁺ restored some level of activity, although Mg²⁺ and Fe²⁺ restored little to no activity. Addition of 100 μM Zn²⁺ restored the highest level of proteolytic activity to the membrane, although 1 mM Zn²⁺ actually inhibited the proteolysis. A similar effect has been observed previously during reconstitution with Zn²⁺ of the zinc metalloprotease, carboxypeptidase A. The inhibition was presumably due to the formation of an inhibitory ZnOH⁺ complex (41), and later confirmed by the x-ray crystal structure of the inhibited enzyme (42).

One of the more perplexing results was the high level of reconstitution with Ca²⁺, which normally restores little to no activity when substituted into zinc metalloproteases. The fact that it is a hard metal ion and its preference for 6–8 ligands make Ca²⁺ seem an unlikely guest in a site optimized for Zn²⁺. In enzymes, Zn²⁺ is usually coordinated by less than six ligands; the relative ease with which Zn²⁺ moves between 4- and 6-coordinate complexes allows it to serve as a catalyst in several enzyme mechanisms (e.g. carboxypeptidase A). Furthermore, Zn²⁺ is often found coordinated to histidine and cysteine residue through nitrogen and sulfur atoms, respectively. Such a coordination sphere is strongly disfavored by the hard metal ion Ca²⁺. The Ca²⁺ effect may be due to the presence of a Ca²⁺-activated protease in the thylakoid membrane, with the reconstitution of activity arising from the presence of trace amounts of Zn²⁺ in the CaCl₂ stock solution. However, if this were the case, other metals such as Zn²⁺ and Co²⁺ would likely not restore such a high level of activity in the absence of Ca²⁺. There are examples of proteases in several different classes that require Ca²⁺ for activity: Zn²⁺-metalloproteases (e.g. thermolysin (43)), cysteine proteases (e.g. calpains (44)), and serine proteases (e.g. furin) (45)). The presence of such a non-metalloprotease as an obligatory actor seems unlikely in this system, due to the inability of several non-metalloprotease inhibitors to decrease activity and the high degree of reconstitution with even small amounts of Zn²⁺. One hypothesis that could explain these disparate observations is that there is more than one metal-dependent protease capable of degrading PS1 in chloroplast membranes. EDTA inhibits all of them, and the activity of at least one is restored by Zn²⁺/Co²⁺, although the other(s) are restored by Ca²⁺.

Attempts to discriminate between activation by Ca²⁺ and Zn²⁺ were made using the metal chelator 1,10-*o*-phenanthroline. The idea was to add *o*-phenanthroline to an *in vitro* assay at a concentration significantly lower than that of the normal Ca²⁺ concentration (2 mM). If degradation of PS1 were inhibited, this would likely indicate that *o*-phenanthroline had chelated the native Zn²⁺, although no inhibition might indicate that the presence of Ca²⁺ alone is sufficient for enzymatic activity. The fact that *o*-phenanthroline increased the rate of PS1 degradation (data not shown) leaves this question unanswered. Experiments using *o*-phenanthroline and its nitrogenless analogue phenanthrene suggested that the increased degradation of PS1 in the presence of *o*-phenanthroline is likely due to the hydrophobic nature of this compound rather than its metal-chelating properties (data not shown). Although *o*-phenanthroline is an effective inhibitor of metal proteases in aqueous systems, it probably partitions into membranes. Insertion between trans-membrane α-helices of PS1 could perturb its structure, rendering it a better substrate for the disassembly/degradation machinery. The fact that this degradation remained dependent upon the presence of divalent cations (data not shown) suggests that the usual proteolytic system was still operative in the presence of *o*-phenanthroline. This is a dramatic demonstration of the difference between working on soluble and membrane protein substrates.

The appearance of a 115-kDa band in the later time points was often seen in anti-PsaA immunoblots. It may represent some kind of cross-linked product, but not disulfide-linked, as the samples were reduced with DTT. In addition, the 115-kDa band does not accumulate at all in the presence of trypsin and chymotrypsin, suggesting that it is particularly susceptible to proteolysis. Whether this band represents an intermediate product in the normal PS1 degradation pathway or is an artifact from the *in vitro* system not on the pathway to complete degradation is unclear at this time.

Acknowledgment—We thank Kristin Brunelle for the initial work in helping to create the system.

REFERENCES

1. Wiley, H. S. (1985) *Curr. Top. Membr. Transp.* **24**, 369–412
2. Rivett, A. J. (1990) *Curr. Opin. Cell Biol.* **2**, 1143–1149
3. Hershko, A., and Ciechanover, A. (1992) *Annu. Rev. Biochem.* **61**, 761–807
4. Akabas, M. H. (2000) *J. Biol. Chem.* **275**, 3729–3732
5. Kopito, R. R. (1999) *Physiol. Rev.* **79**, 167–173
6. Vekrellis, K., Ye, Z., Qiu, W. Q., Walsh, D., Hartley, D., Chesneau, V., Rosner, M. R., and Selkoe, D. J. (2000) *J. Neurosci.* **20**, 1657–1665
7. McDermott, J. R., and Gibson, A. M. (1997) *Neurochem. Res.* **22**, 49–56
8. Berson, E. L. (1996) *Proc. Natl. Acad. Sci. U. S. A.* **93**, 4526–4528
9. Rochaix, J. D. (1992) *Annu. Rev. Cell Biol.* **8**, 1–28
10. Choquet, Y., and Vallon, O. (2000) *Biochimie (Paris)* **82**, 615–634
11. Ostersetzer, O., Tabak, S., Yarden, O., Shapira, R., and Adam, Z. (1996) *Eur. J. Biochem.* **236**, 932–936
12. Lindahl, M., Tabak, S., Cseke, L., Pichersky, E., Andersson, B., and Adam, Z. (1996) *J. Biol. Chem.* **271**, 29329–29334
13. Cook, M., and Adam, Z. (1997) *Plant Physiol. Biochem.* **35**, 163–168
14. Itzhaki, H., Naveh, L., Lindahl, M., Cook, M., and Adam, Z. (1998) *J. Biol. Chem.* **273**, 7094–7098
15. Rüfenacht, A., and Boschetti, A. (2000) *Photosynth. Res.* **63**, 249–258
16. Lensch, M., Herrmann, R. G., and Sokolenko, A. (2001) *J. Biol. Chem.* **276**, 33645–33651
17. Halperin, T., Ostersetzer, O., and Adam, Z. (2001) *Planta* **213**, 614–619
18. Adam, Z., Adamska, I., Nakabayashi, K., Ostersetzer, O., Haussuhl, K., Manuell, A., Zheng, B., Vallon, O., Rodermeil, S. R., Shinozaki, K., and Clarke, A. K. (2001) *Plant Physiol.* **125**, 1912–1918
19. Majeran, W., Wollman, F. A., and Vallon, O. (2000) *Plant Cell* **12**, 137–150
20. Majeran, W., Olive, J., Drapier, D., Vallon, O., and Wollman, F. A. (2001) *Plant Physiol.* **126**, 421–433
21. Spetea, C., Hundal, T., Lohmann, F., and Andersson, B. (1999) *Proc. Natl. Acad. Sci. U. S. A.* **96**, 6547–6552
22. Ostersetzer, O., and Adam, Z. (1997) *Plant Cell* **9**, 957–965
23. Kihara, A., Akiyama, Y., and Ito, K. (1999) *EMBO J.* **17**, 50–60
24. Jordan, P., Fromme, P., Witt, H. T., Klukas, O., Saenger, W., and Krauss, N. (2001) *Nature* **411**, 909–917
25. Harris, E. H. (1989) *The Chlamydomonas Sourcebook. A Comprehensive Guide to Biology and Laboratory Use*, pp. 25–40, Academic Press, San Diego
26. Porra, R., Thompson, W., and Kriedemann, P. (1989) *Biochim. Biophys. Acta* **975**, 384–394
27. Redding, K., Macmillan, F., Leibl, W., Brettel, K., Hanley, J., Rutherford, A. W., Breton, J., and Rochaix, J.-D. (1998) *EMBO J.* **17**, 50–60
28. Boudreaux, B., MacMillan, F., Teutloff, C., Agalarov, R., Gu, F., Grimaldi, S., Bittl, R., Brettel, K., and Redding, K. (2001) *J. Biol. Chem.* **276**, 37299–37306
29. Hall, D. O., and Rao, K. K. (1994) *Photosynthesis*, 5th Ed., pp. 10–11, Cambridge University Press, Cambridge, UK
30. Caspi, V., Malkin, S., and Marder, J. B. (2000) *Photochem. Photobiol.* **71**, 441–446
31. Murakami, A. (1997) *Photosynth. Res.* **53**, 141–148
32. Thornber, J. P., Gregory, R. P., Smith, C. A., and Bailey, J. L. (1967) *Biochemistry* **6**, 391–396
33. Warren, P. V., Parrett, K. G., Warden, J. T., and Golbeck, J. H. (1990) *Biochemistry* **29**, 6545–6550
34. Tomoyasu, T., Yamanaka, K., Murata, K., Suzuki, T., Bouloc, P., Kato, A., Niki, H., Hiraga, S., and Ogura, T. (1993) *J. Bacteriol.* **175**, 1352–1357
35. Tomoyasu, T., Gamer, J., Bukau, B., Kanemori, M., Mori, H., Rutman, A. J., Oppenheim, A. B., Yura, T., Yamanaka, K., and Niki, H. (1995) *EMBO J.* **14**, 2551–2560
36. Breddam, K., Bazzzone, T. J., Holmquist, B., and Vallee, B. L. (1979) *Biochemistry* **18**, 1563–1570
37. Bünning, P., and Riordan, J. F. (1985) *J. Inorg. Biochem.* **24**, 183–198
38. Angleton, E. L., and Van Wart, H. E. (1988) *Biochemistry* **27**, 7413–7418
39. Stoecker, W., Wolz, R. L., Zwilling, R., Strydom, D. J., and Auld, D. S. (1988) *Biochemistry* **27**, 5026–5032
40. Zisapel, N., and Sokolovsky, M. (1993) *Biochem. Biophys. Res. Commun.* **53**, 722–729
41. Larsen, K. S., and Auld, D. S. (1991) *Biochemistry* **30**, 2613–2618
42. Gomez-Ortiz, M., Gomis-Ruth, F. X., Huber, R., and Aviles, F. X. (1997) *FEBS Lett.* **400**, 336–340
43. Roche, R. S., and Voordouw, G. (1978) *CRC Crit. Rev. Biochem.* **5**, 1–23
44. Hosfield, C. M., Elce, J. S., Davies, P. L., and Jia, Z. (1999) *EMBO J.* **18**, 6880–6889
45. Fuller, R. S., Brake, A., and Thornber, J. (1989) *Proc. Natl. Acad. Sci. U. S. A.* **86**, 1434–1438